TOPICAL REVIEW — Interface-induced high temperature superconductivity

Direct evidence of high temperature superconductivity in one-unit-cell FeSe films on $SrTiO_3$ substrate by transport and magnetization measurements*

Xing Ying(邢 颖)[a)b)] and Wang Jian(王 健)[a)b)†]

[a)] International Center for Quantum Materials, School of Physics, Peking University, Beijing 100871, China
[b)] Collaborative Innovation Center of Quantum Matter, Beijing 100871, China

(Received 30 June 2015; published online 9 October 2015)

Zero resistance and Meissner effect are two crucial experimental evidences of superconductivity in determining a new kind of superconductor, which can be detected by transport and diamagnetic measurements. In this paper, we briefly review the main transport and magnetization results on the one unit cell (1-UC) FeSe films grown on $SrTiO_3$ (STO) substrates from our team in recent years, which identify the high temperature superconductivity in 1-UC FeSe films.

Keywords: two-dimensional superconductivity, one-unit-cell FeSe, transport measurement, diamagnetic property

PACS: 74.78.–w, 73.61.–r, 73.63.–b, 75.75.–c **DOI:** 10.1088/1674-1056/24/11/117404

1. Introduction

The discovery of superconductor $La[O_{1-x}F_x]FeAs$ ($x = 0.05$–0.12) with transition temperature (T_c) of 26 K in 2008[1] triggered an impressive amount of experimental and theoretical studies in condensed matter physics and material science.[2–7] It is unexpected that superconductivity exists in compounds which contain the element Fe since normally ferromagnetism is against superconductivity. Therefore, this discovery causes worldwide effort to understand the nature of the superconductivity in iron-based superconductors. So far, four basic types have been discovered: LaFeAsO "1111" type,[8] MFe_2As_2 "122" type,[9] MFeAs "111" type,[10] and FeSe "11" type,[11] with the maximum T_c climbing as high as 55 K[5] and 56 K[12,13] in the bulk materials. Similar to cuprates, the naturally layered iron based superconductor has been demonstrated as another high temperature superconductor.

When one dimension of a bulk superconductor decreases to smaller than the coherence length of the Cooper pairs, the superconductor can be considered as a quasi-two dimensional (quasi-2D) superconductor.[14] Due to thermo and quantum fluctuations, which are more severe in the low dimensional system, the superconductivity should be suppressed by decreasing the thickness of a superconducting film, which has been confirmed by many groups.[15–17] However, for quasi-2D superconductors epitaxially grown on substrates, the interface may promote T_c by enhancing the electron–phonon coupling[18] and the epitaxial strain.[19] Recently, atomically flat one unit cell (1-UC) thick β-FeSe films have been successfully grown on STO (001) substrates by molecular beam epitaxy (MBE) technique.[20] For the 1-UC FeSe on STO, a superconducting-like energy gap as large as 20 meV obtained from *in situ* scanning tunneling spectra (STS)[20] or 15 meV (disappear at 65 ± 5 K) detected by *in situ* angle-resolved photoemission spectroscopy (ARPES)[21,22] was observed, which is much larger than $\Delta \sim 2.2$ meV for bulk FeSe ($T_c \sim 8$ K at ambient pressure[11]). Then, the key question for these observations is if the observed gap in the 1-UC FeSe films is really the superconducting gap. Thus, the direct evidences of zero resistance and the Meissner effect are necessary to demonstrate the enhanced superconductivity in the 1-UC FeSe films.

For the *ex situ* transport and diamagnetic measurements, the 1-UC FeSe films must be taken out of the ultrahigh vacuum (UHV) system. Since the atmosphere condition can easily destroy the superconductivity in such thin films, only 5-UC FeSe films covered by amorphous Si protection layer (20 nm) were measured[20] before our work of *ex situ* transport measurements. Although the superconducting transition in resistance for 5-UC FeSe was observed, the zero resistance was not detected. Therefore, to surely determine the superconductivity of the 1-UC FeSe films by *ex situ* measurements is quite challenging but very important.

Here, the zero resistance and the Meissner effect evidences of high temperature superconductivity in 1-UC FeSe films with enhanced T_c, upper critial field H_{c2}, and critical current density J_c, detected by *ex situ* transport and magnetization measurements, which were firstly reported by our team, are reviewed.

*Project supported by the National Basic Research Program of China (Grant Nos. 2013CB934600 and 2012CB921300), the National Natural Science Foundation of China (Grant Nos. 11222434 and 11174007), and the Research Fund for the Doctoral Program of Higher Education (RFDP) of China.

†Corresponding author. E-mail: jianwangphysics@pku.edu.cn

© 2015 Chinese Physical Society and IOP Publishing Ltd

2. Transport and diamagnetic properties of 1-UC FeSe on intrinsic STO

The 1-UC β-FeSe films (a Se–Fe–Se triple layer with thickness of 0.55 nm) were synthetized by an MBE system, starting from Fe and Se powders with a flux ratio of 1:10 on the STO(001) substrates.[23] The atomically flat 1-UC FeSe film (Fig. 1(a)), with in-plane lattice constants $a = b = 3.82$ Å, has a lattice mismatch of 2.36% with the STO substrate (3.91 Å). The 1-UC FeSe is too thin to survive in the atmosphere. So searching for a suitable protecting layer is a significant step for *ex situ* studies. In our measurements, non-superconducting FeTe layers (10 UC) were chosen to cover the 1-UC FeSe film by MBE since FeTe can be epitaxially grown on the FeSe film and protect the FeSe film well. Figures 1(b) and 1(c) show scanning transmission electron microscope (STEM) images of two sharp interfaces from the cross-section of the FeTe/FeSe/STO heterostructure, which demonstrate the good quality of the 1-UC FeSe film after depositing the protection layer. For further protection, an amorphous Si film is used as the second cover layer grown on the FeTe film to avoid oxygen incorporation into the FeTe film and further protect the FeSe sample.

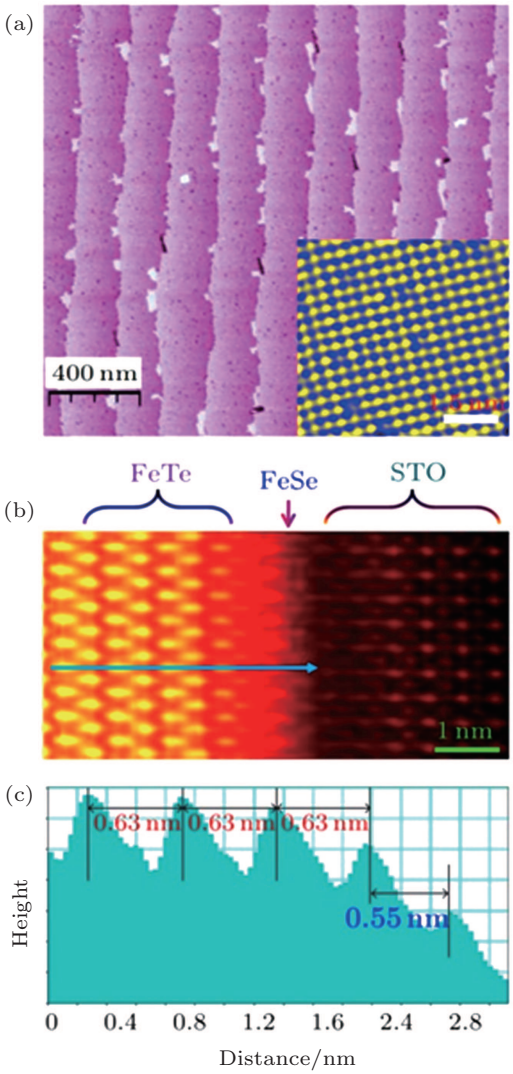


Fig. 1. (a) STM image of a typical 1-UC FeSe film. The steps originate from the STO substrate and the inset shows the atomic-resolution image. (b) The high-angle annular dark field STEM image of a (10-UC)FeTe/(1-UC)FeSe/STO heterostructure, showing two very sharp interfaces. (c) The line profile corresponding to the blue line in panel (b), confirming the distinct FeTe cover layer, the FeSe film, and the $SrTiO_3$ substrate.[23]

2.1. Robust superconductivity in 1-UC FeSe film

For transport measurements, standard four-electrode or six-electrode measurements were used for the Si/(10-UC)FeTe/(1-UC)FeSe/STO heterostructure with an area of ~ 8 mm$\times 1.5$ mm (see the inset of Fig. 2(a)). The temperature dependence of resistance under zero magnetic field exhibits an obvious onset superconducting drop with $T_c^{onset} \sim 54.5$ K (Fig. 2(a)) and the resistance drops to zero (within the instrumental noise limit, here ± 20 nV) at 23.5 K (T_c^{zero}). The corresponding magnetization measurement of this heterostructure also exhibits a sharp drop around 25 K (labeled by the red arrow in Fig. 2(b)), close to $T_c^{zero} \sim 23.5$ K in the $R(T)$ curve. The typical magnetic hysteresis loop measured at 2 K further confirms the superconductivity of the heterostructure. To verify the origin of the superconductivity, the same transport measurements were carried out for the STO substrate and the heterostructures of (10-UC)FeTe /STO and Si/(10-UC)FeTe/STO, respectively, and they all exhibit insulating-like behaviors (Figs. 2(c) and 2(d)). Moreover, the STS data also prove that the superconducting-like gap only exists in the first FeSe layer on STO. The typical dI/dV spectra taken on the 1st-UC FeTe, the 2nd-UC FeTe (Figs. 3(a) and 3(c)) on 1-UC FeSe film, the exposed Nb-doped STO surface (Figs. 3(b) and 3(d)) under 1-UC FeSe, and even the 2nd FeSe layer for a 2-UC FeSe film on STO[20] exhibit non-superconducting properties.[23] The above experiments clearly identify that the superconductivity is limited in the 1-UC FeSe films and the proximity effect[24–26] cannot make the substrate and the protection layer superconducting. Therefore, the 1-UC FeSe with the thickness of 0.55 nm grown on STO should be the thinnest high temperature superconductor discovered so far. Soon after our work, a systematic investigation on the superconductivity in 1-4 UC FeSe films by susceptibility measurement as a function of temperature and frequency was reported.[27] Their results show that the FeSe films on STO display a complex superconducting structure: a Meissner state but populated with weak links below 20 K, and an unusual superconducting mesostructure up to 45 K.[27]

We would like to mention that the indium electrodes we used can easily penetrate through the protection layers (here ~ 50 nm thick) and connect the FeSe film by directly pressing the electrodes on the top surface of the Si/(10-UC)FeTe/(1-UC)FeSe/STO heterostructure. Thus, it is not surprising *ex situ* transport and diamagnetic measurements reveal the superconductivity in multi-UC FeSe films,[23,27] although the STM data shows non-superconducting behavior for the top surface of the multi-UC FeSe film.[20] Based on the above discussion, we believe that only the first UC FeSe on STO superconducts even that the FeSe film is multi-UC thick.

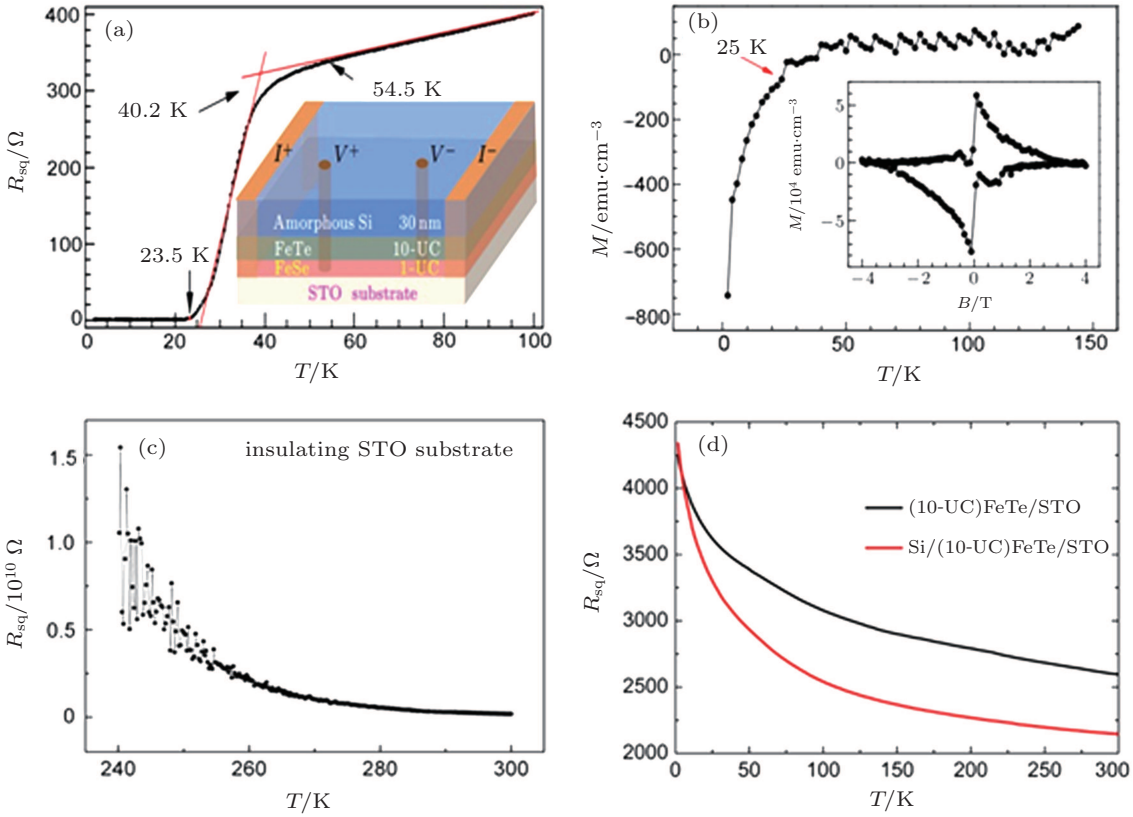


Fig. 2. (a) The $R(T)$ curve of superconducting Si/(10-UC)FeTe/(1-UC)FeSe/STO heterostructure, showing $T_c^{onset} = 54.5$ K and $T_c^{zero} = 23.5$ K. The inset is a schematic structure for standard four-electrode measurement. (b) Temperature dependence of magnetization for 1-UC FeSe film on intrinsic STO measured at a parallel field of 1000 Oe. Typical magnetic hysteresis loop is shown in the inset. Insulating-like properties of the STO substrate, 10-UC FeTe/STO, and Si/10-UC FeTe/STO heterostructures are shown in panels (c) and (d), respectively.[23]

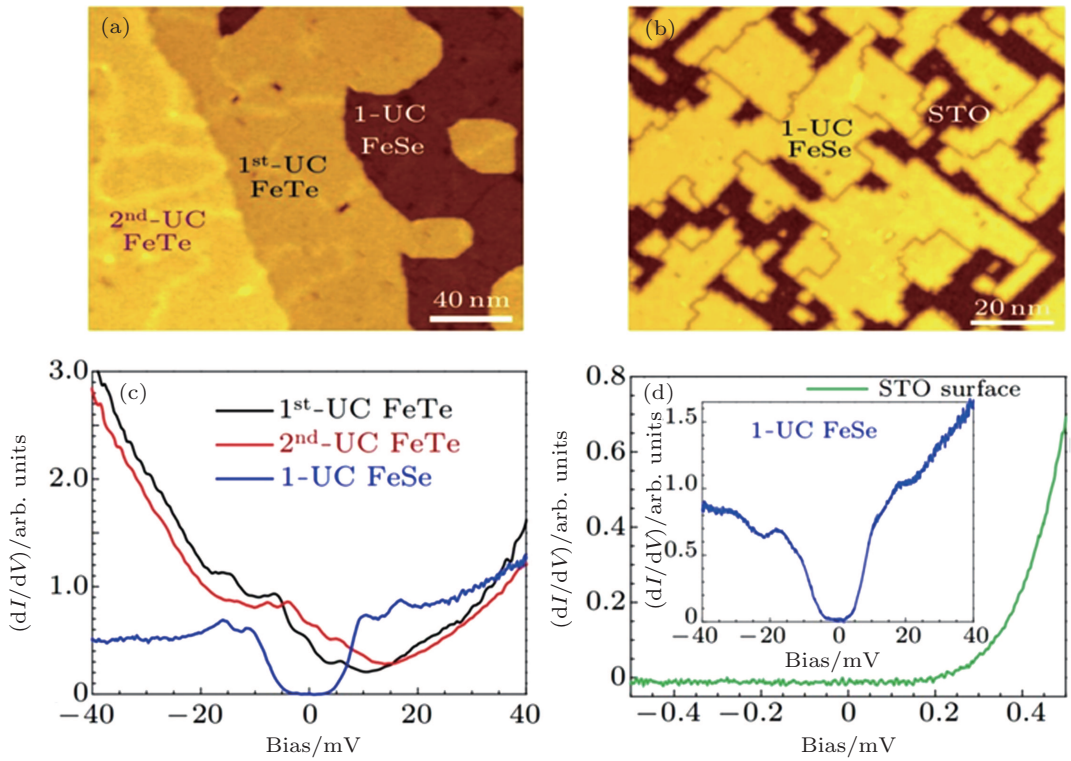


Fig. 3. (a) STM image of 1-UC FeSe film partially covered by the (1-UC & 2-UC) FeTe protection layer on conductive STO substrate. (b) STM image of the 1-UC FeSe film with some parts of the STO surface exposed. (c) The typical dI/dV spectra taken on the 1st-UC FeTe, the 2nd-UC FeTe, and the 1-UC FeSe films. (d) The typical dI/dV spectra taken on 1-UC FeSe film and exposed STO surface.[23]

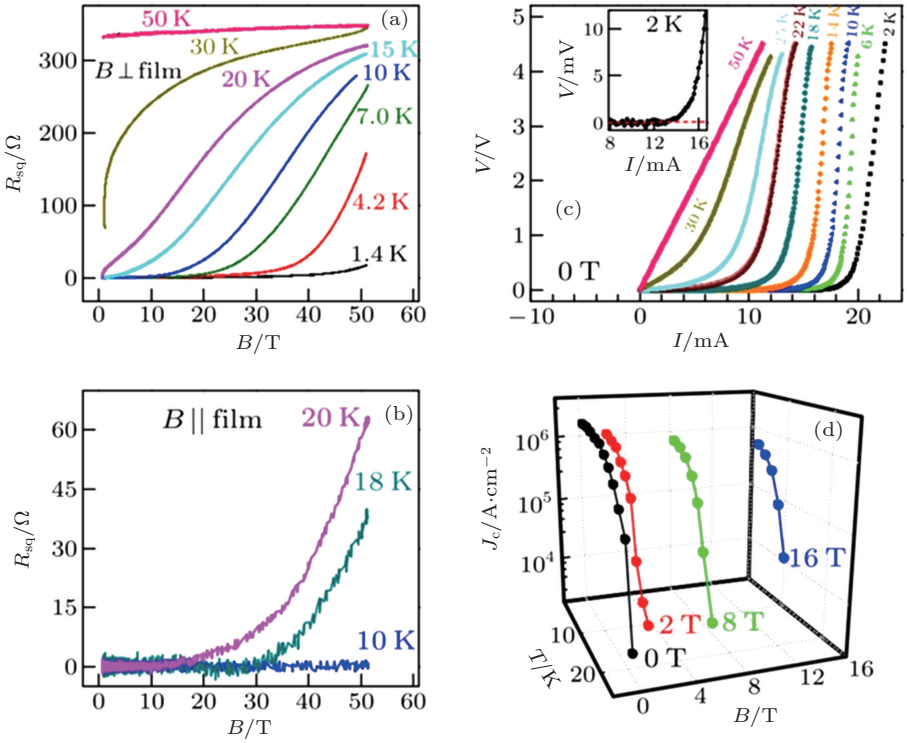


Fig. 4. Characterization of the superconductivity. Magnetoresistance measured in (a) perpendicular and (b) parallel magnetic fields with pulsed magnetic field up to 52 T. (c) The $V(I)$ curves measured at temperatures ranging from 2 K to 50 K in zero magnetic field. (d) The J_c calculated from I_c at various temperatures and perpendicular magnetic fields.[23]

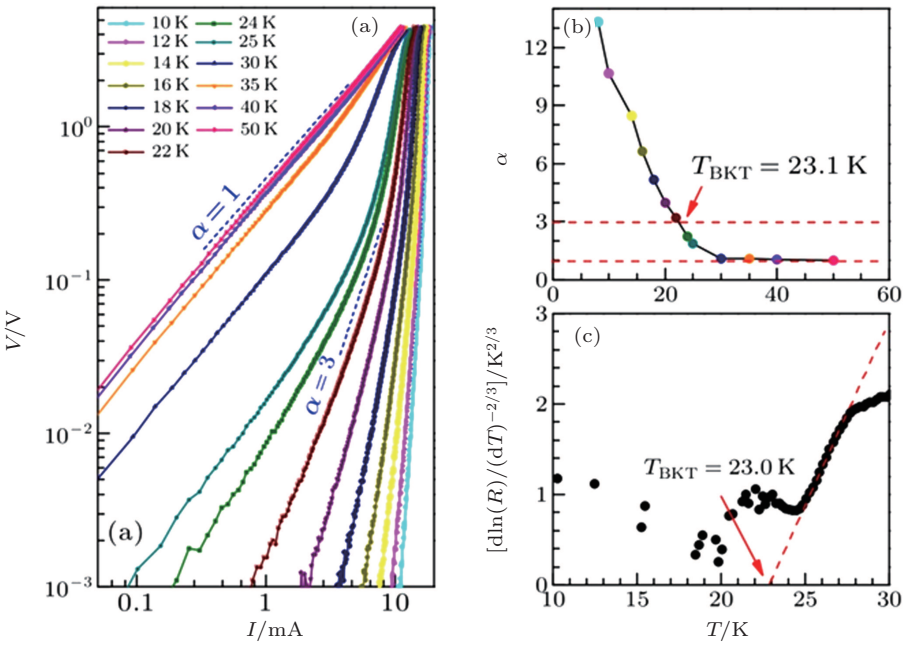


Fig. 5. BKT like transition of 1-UC FeSe films. (a) The $V(I)$ curves at different temperatures, the two dashed lines correspond to $V \sim I$ and $V \sim I^3$. (b) The power-law exponent α ($V \sim I^{\alpha}$) as a function of temperature, with $\alpha = 3$ ($T \sim 23.1$ K) indicating BKT transition. (c) The $R(T)$ curve plotted on a $[\mathrm{d}\ln(R)/\mathrm{d}T]^{-2/3}$ scale. The dashed line is the behavior expected for a BKT transition with $T_{BKT} = 23.0$ K.[23]

To determine H_{c2} of the 1-UC FeSe film, pulsed high magnetic fields up to 52 T were applied perpendicular and parallel to the film (Figs. 4(a) and 4(b)) for the measurements. Anisotropic and robust superconductivity is observed. In the perpendicular magnetic field, the sample remains in the zero resistance state until the field increases to 40 T at 1.4 K. Even 52 T can hardly tune the film to its normal state, unless the temperature is near T_c. As for the parallel field situation, at 10 K, the sample shows zero resistance up to 52 T, revealing a much higher critical magnetic field than that in the perpendicular situation. This observation is consistent with the anisotropic behavior of a typical 2 D superconductor. The

$H_{c2}(0)$ is estimated to be 37 T for bulk FeSe, and is increased from 37 T to 72 T by applying a pressure of 1.48 GPa.[28] Therefore, the estimated value ($\sim$ 80 T) of perpendicular critical field H_{c2} in the 1-UC FeSe/STO system is enhanced compared to that of bulk FeSe.

In addition, the thin FeSe superconducting film shows an unexpected large critical current. The zero field voltage versus current ($V(I)$) curves at various temperatures are exhibited in Fig. 4(c). At 2 K, the critical current is as large as 13.3 mA, as shown in the inset. The derived temperature and magnetic field dependences of J_c for the 1-UC FeSe film are shown in Fig. 4(d) by considering the thickness of 0.55 nm of the superconducting layer as we confirmed above. At 2 K, J_c is 1.7×10^6 A/cm^2, which is one order of magnitude higher than that of $FeTe_{0.61}Se_{0.39}$ crystal[29] and two orders larger than that of bulk FeSe ($J_c \sim 10^4$ A/cm^2).[30]

The signature of Berezinski–Kosterlitz–Thouless (BKT) like behavior is observed in the 1-UC FeSe film as another evidence of 2D superconductivity.[31,32] As shown in Fig. 5(a), the $V(I)$ curves of 1-UC FeSe just below I_c can be fitted by a power-law dependence ($V \propto I^{\alpha}$). Figure 5(b) reveals that the exponent α approaches 3 at $T = 23.1$ K. This temperature is therefore identified as T_{BKT}. Furthermore, the BTK-like fitting for $R(T)$ characteristics (Fig. 5(c)) also indicates a T_{BKT} of 23.0 K, which is consistent with the fitting result from the $V(I)$ curves.

2.2. Arrhenius thermally activated flux flow behavior

For a typical type-II superconductor, the dissipation behavior is influenced by the competition beteween the pinning forces (the pinning force dominated flux creep regime) and the Lorentz force (the Lorentz force dominated flux flow regime) in an external magnetic field. To evaluate the extent to which formalism is applicable for our 1-UC FeSe films, the resistance versus temperature curves of the 1-UC FeSe film in various magnetic fields were measured (Fig. 6(a)).[33] Figure 6(b) reveals the corresponding $\ln[R_{sq}]$ vs. $1/T$ relations. The thermally activated flux flow (TAFF) of the vortex region can be described by the Arrhenius relation: $\rho(T,H) = \rho(H)\exp[-U_0(H)/T]$, where U_0 is the activation energy in the absence of a gradient.[34] Linear fits are performed on the low-temperature part (large $1/T$ behavior), which are shown as solid pink lines. The slopes obtained from these fits yield the activation energies $U_0(H)$ in various magnetic fields (see Fig. 6(c)). The plots of $\ln[R_{sq}]$ vs. $1/T$ for various fields have a common intersection point, which should ideally correspond to the T_c of the superconducting specimen. In this sample, the intersection point corresponds to a temperature of $T_m \sim 38$ K, which is close to the middle point T_c from the R_{sq} vs. T curves. Besides, power-law fits ($H^{-\gamma}$) are performed on the $U_0(H)$ data and the two regimes are clearly visible with a crossover occurring at a characteristic field $\mu_0 H$ (≈ 3.4 T), with different exponents γ on the two sides ($\gamma = 0.14$ for $\mu_0 H < 3.4$ T and 0.60 for $\mu_0 H > 3.4$ T). A change in the exponent γ by about a factor of 4 across $\mu_0 H$ with a relatively small value at low field suggests a crossover from a single-vortex pinning dominated regime to a collective flux creep regime across $\mu_0 H$. Similar crossover behaviors have been found in β-FeSe ($\mu_0 H \approx 3$ T)[30] and $SmFeAsO_{0.85}$ ($\mu_0 H \approx 3T$)[35] bulk crystals.

2.3. Sign reversal of Hall coefficient

The nature of charge carriers in the normal state is one of the crucial ingredients which are required to understand the mechanism of superconductivity. We performed Hall effect measurements for the 1-UC FeSe films. The electronic contacts for the Hall measurements were made in 6-electrode geometry by using indium spheres and 25 μm diameter gold wires. The Hall resistance (R_{xy}) was obtained by sweeping the magnetic field at a fixed temperature. The R_{xy} vs. magnetic field curves at different temperatures (Figs. 7(a) and 7(d)) exhibit a good linear relation. For the two FeSe films we studied, T_c^{onset} are around 45.8 K and 54.5 K, respectively. After subtracting the contribution of the FeTe protection layer (Figs. 7(b) and 7(e)), the observed Hall coefficient and carrier density of 1-UC FeSe as a function of temperature are shown

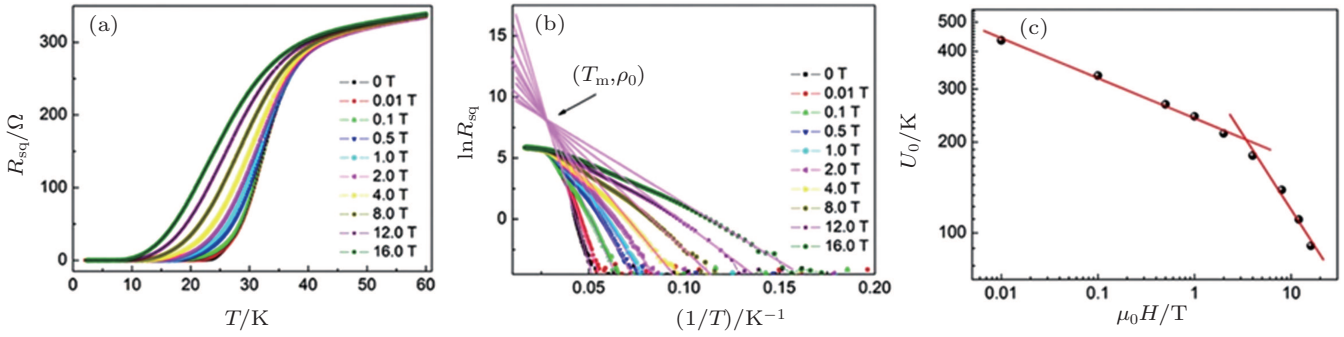


Fig. 6. Arrhenius TAFF analysis. (a) Temperature dependence of resistance in different magnetic fileds. (b) $\ln[R_{sq}]$ vs. $1/T$ in various perpendicular magnetic fields. The corresponding solid lines are fitting results from the Arrhenius relation. (c) Field dependence of $U_0(H)$. The solid lines are power-law fits using $U_0(H) \sim H^{-\gamma}$. For this 1-UC FeSe film, $\gamma = 0.14$ for $\mu_0 H < 3.4$ T, and $\gamma = 0.60$ for $\mu_0 H > 3.4$ T.[33]

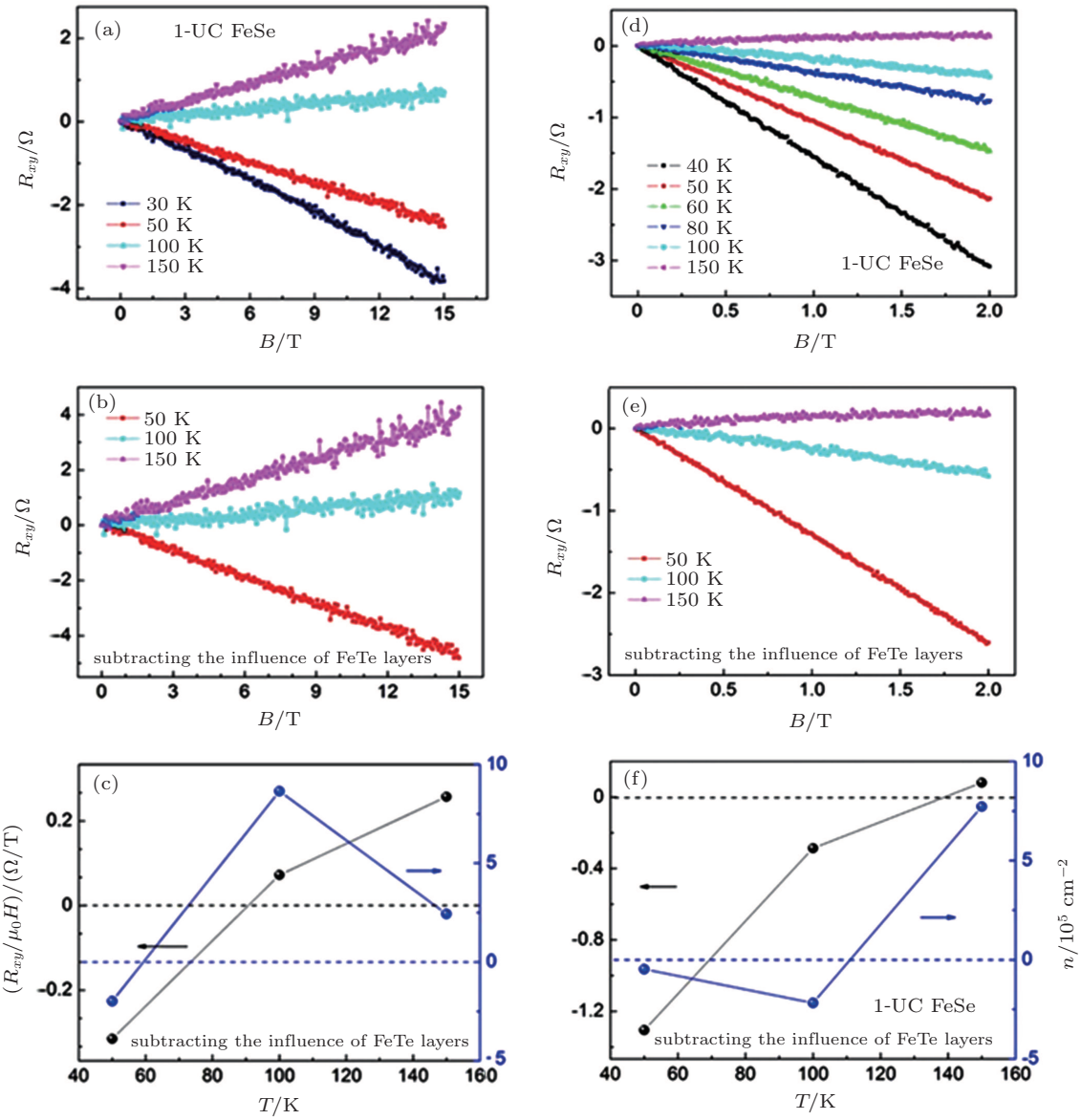


Fig. 7. Hall results of 1-UC FeSe films grown on intrinsic STO substrate. The $R_{xy}(H)$ curves at different temperatures of 1-UC FeSe film without (a) and with (b) subtracting the background. (c) Hall coefficient and the carrier density calculated from data in panel (b). (d)–(f) Data from another 1-UC FeSe sample.[33]

in Figs. 7(c) and Fig. 7(f). Although there are only three T-dependent data points, it is evident that the Hall coefficient is negative at the low temperature of 50 K, pointing to a prominence of electron-like charge carriers in this region. While at 100 K and 150 K, the change of sign is obvious, pointing to hole-like charge carriers in the higher temperature regime.

A similar Hall coefficient sign reversal behavior has also been found in bulk $FeTe_{0.6}Se_{0.4}$[36] and $FeCr_{0.02}Se$,[37] which is usually interpreted by the multiband effect of the electronic structure and the coexistence of electron and hole carriers with different contributions from various bands. This Hall coefficient sign reversal behavior has also been investigated with different annealing time and the characteristic temperature (T_{e-h}) increases with annealing time,[38] indicating a close relationship between superconductivity and the nature of the charge carriers.

3. A hint of T_c above liquid nitrogen temperature in 1-UC FeSe films on conductive (Nb-doped) STO

Compared with *in situ* STM (estimated $T_c \sim 80$ K)[20] and ARPES (estimated $T_c \sim 65$ K)[21,22] data on 1-UC FeSe films growing on conductive STO substrates, our *ex situ* measurements of the FeSe films on intrinsic STO substrates exhibit relatively lower transition temperature with $T_c^{onset} \sim 54.5$ K and $T_c^{zero} \sim 23.5$ K. Indeed, the STM results reveal that high quality FeSe films are easier to be achieved by MBE growth on conductive STO substrates compared to intrinsic STO substrates since the conductive STO substrate shows more flat and homogeneous surface for film growth. As for *ex situ* Meissner effect measurments, the FeSe films grown on intrinsic STO substrates only exhibit transition temperatures of 25 K and 20 K for 1-UC[23] and 3-4 UC[27] FeSe films.

However, the *ex situ* diamagnetic property of FeSe films on conductive STO substrates measured by our group indicates a hint of T_c above the liquid nitrogen temperature.[33,39] The magnetic characterization of a 1-UC FeSe film grown on conductive STO substrate under a parallel magnetic field of 1000 Oe is shown in Fig. 8(a). The data are shown for the zero-field cooled (ZFC) and field cooled (FC) modes. After subtracting the signal from the protection layer and the substrate, we find a diamagnetic drop below $T \sim 85$ K which may correspond to superconductivity (Fig. 8(b)). This is nearly ten times larger than the T_c of bulk FeSe and even higher than the record value of $T_c \sim 56$ K[12,13] in bulk iron-based superconductors. However, the unusual phenomenon that the diamagnetic signal in FC mode is stronger than that in ZFC mode still remains unclear. We will leave this for further investigation.

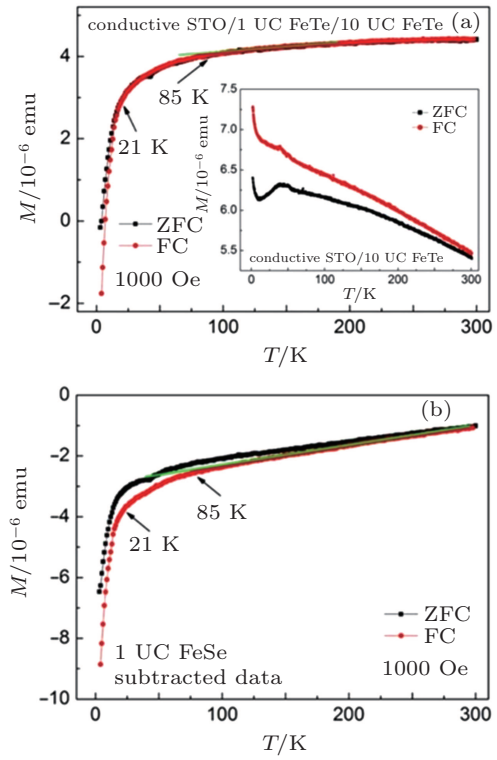


Fig. 8. Diamagnetic measurements of 1-UC FeSe films grown on conductive STO substrate. (a) Data shown for ZFC and FC measurements in 1000 Oe parallel magnetic field. Inset: the $M(T)$ curves of conductive STO/non-superconducting 1-UC FeSe/10-UC FeTe. (b) The $M(T)$ curves of 1-UC FeSe (subtracting the influence of STO substrate and FeTe protection layer).[33]

One recent work also reported the indication of superconductivity with T_c above liquid nitrogen temperature (even larger than 100 K) in FeSe/conductive STO system by means of *in situ* four-point probe (4PP) electrical transport measurement, which is much higher than the observed T_c by *ex situ* standard transport measurment in our work. One possible reason is that our 1-UC FeSe film is covered by a protective FeTe layer, which is known to be antiferromagnetic and may diminish T_c. Although there might be some pitfalls regarding the 4PP method,[39,40] both *in situ* transport measurement and *ex situ* magnetization measurement show a hint that the FeSe/STO structure might become the second system with transition temperature higher than the boiling point of liquid nitrogen, while confirmatory experiments like *in situ* diamagnetic and standard four-electrode transport measurements are required to fully confirm this.

The understanding of extremely enhanced superconductivity in 1-UC FeSe films has attracted a tremendous amount of attention over the past few years. Why do Cooper pairs form at such high temperatures? What is the possible physical mechanism in this system? One recent high-resolution ARPES study[41] reveals shake-off bands in the 1-UC FeSe/STO system, suggesting the presence of bosonic modes. Such a mode may come from the interaction between oxygen optical phonons in STO and electrons in FeSe. It is suggested that this coupling is responsible for raising the opening temperature of the superconducting gap in 1-UC FeSe/STO.

4. Summary

The key experimental evidences of superconductivity in 1-UC FeSe films on STO substrates by *ex situ* transport and diamagnetic measurements are briefly reviewed. The interface enhanced superconductivity with high T_c, H_c, and J_c makes the FeSe ultra-thin films not only interesting for detecting and understanding high temperature superconductivity but also attractive for potential applications in superconducting electronics. We hope the studies in FeSe/STO heterostructures will open a door for exploring new unconventional superconductors by interface engineering.

Acknowledgment

We are grateful for all our collaborators for materials fabrication, helpful discussion, and experimental support.

References

[1] Kamihara Y, Watanabe T, Hirano M and Hosono H 2008 *J. Am. Chem. Soc.* **130** 3296
[2] Chen X H, Wu T, Wu G, Liu R H and Fang D F 2008 *Nature* **453** 761
[3] Chen G F, Li Z, Wu D, Li G, Hu W Z, Dong J, Zheng P, Luo J L and Wang N L 2008 *Phys. Rev. Lett.* **100** 247002
[4] Wen H H, Wu G, Fang L, Yang H and Zhu X Y 2008 *Eurrophys. Lett.* **80** 17009
[5] Ren Z A, Lu W, Yang J, Yi W, Shen X L, Li Z C, Che G C, Dong X L, Sun L L, Zhou F and Zhao Z X 2008 *Chin. Phys. Lett.* **25** 2215
[6] Dong J, Zhang H J, Xu G, Li Z, Li G, Hu W Z, Wu D, Chen G F, Dai X, Luo J L, Fang Z and Wang N L 2008 *Eurrophys. Lett.* **83** 27006
[7] Wang F and Lee D H 2011 *Science* **332** 200
[8] Pöttgen R and Johrendt D 2008 *Z. Naturforsch.* **63b** 1135
[9] Rotter M, Tegel M and Johrendt D 2008 *Phys. Rev. Lett.* **101** 107006
[10] Wang X C, Liu Q Q, Lv Y X, Gao W B, Yang L X, Yu R C, Li F Y and Jin C Q 2008 *Solid State Commun.* **148** 538
[11] Hsu F C, Luo J Y, Yeh K W, Chen T K, Huang T W, Wu P M, Lee Y C, Huang Y L, Chu Y Y, Yan D C and Wu M K 2008 *Proc. Natl. Acad. Sci. USA* **105** 14262
[12] Wang C, Li L J, Chi S, Zhu Z W, Ren Z, Li Y K, Wang YT, Lin X, Luo Y K, Jiang S, Xu X F, Cao G H and Xu Z A 2008 *Europhys. Lett.* **83** 67006

[13] Wu, G, Xie Y L, Chen H, Zhong M, Liu R H, Shi B C, Li Q J, Wang X F, Wu T, Yan Y J, Ying J J and Chen X H 2009 *J. Phys.: Condens. Matter* **21** 142203

[14] Singh M, Sun Y and Wang J 2012 *Superconductivity in Nanoscale Systems* chapter 6 (Rijeka: InTech)

[15] Zhao W W, Wang Q Y, Liu M H, Zhang W H, Wang Y L, Chen M, Guo Y, He K, Chen X, Wang Y Y, Wang J, Xie X C, Niu Q, Wang L L, Ma X C, Jain J K, Chan M H and Xue Q K 2013 *Solid State Commun.* **165** 59

[16] Song C L, Wang Y L, Jiang Y P, Li Z, Wang L L, He K, Chen X, Ma X C and Xue Q K 2011 *Phys. Rev. B* **84** 020503(R)

[17] Haviland D B, Liu Y and Goldman A M 1989 *Phys. Rev. Lett.* **62** 2180

[18] Strongin M, Kammetrer O F, Crow J E, Parks R D, Douglass J and Jensen M A 1968 *Phys. Rev. Lett.* **21** 1320

[19] Locquet J P, Perret F, Fompeyrine J, Mächler E, Seo J W and Tendeloo G V 1998 *Nature* **394** 453

[20] Wang Q Y, Li Z, Zhang W H, Zhang Z C, Zhang J S, Li W, Ding H, Ou Y B, Deng P, Chang K, Wen J, Song C L, He K, Jia J F, Ji S H, Wang Y Y, Wang L L, Chen X, Ma X C and Xue Q K 2012 *Chin. Phys. Lett.* **29** 037402

[21] He S L, He J F, Zhang W H, Zhao L, Liu D F, Liu X, Mou D X, Ou Y B, Wang Q Y, Li Z, Wang L L, Peng Y Y, Liu Y, Chen C Y, Yu L, Liu G D, Dong X L, Zhang J, Chen C T, Xu Z Y, Chen X, Ma X C, Xue Q K and Zhou X J 2013 *Nat. Mater.* **12** 605

[22] Tan S H, Zhang Y, Xia M, Ye Z R, Chen F, Xie X, Peng R, Xu D F, Fan Q, Xu H C, Jiang J, Zhang T, Lai X C, Xiang T, Hu J P, Xie B P and Feng D L 2013 *Nat. Mater.* **12** 634

[23] Zhang W H, Sun Y, Zhang J S, Li F S, Guo M H, Zhao Y F, Zhang H M, Peng J P, Xing Y, Wang H C, Fujita T, Hirata A, Li Z, Ding H, Tang C J, Wang M, Wang Q Y, He K, Ji S H, Chen X, Wang J F, Xia Z C, Li L, Wang Y Y, Wang J, Wang L L, Chen MW, Xue Q K and Ma X C 2014 *Chin. Phys. Lett.* **31** 017401

[24] Binnig G, Baratoff A, Hoenig H E and Bednorz J G 1980 *Phys. Rev. Lett.* **45** 1352

[25] Lin X, Bridoux G, Gourgout A, Seyfarth G, Kramer S, Nardone M, Fauque B and Behnia K 2014 *Phys. Rev. Lett.* **112** 207002

[26] Wang J, Singh M, Tian M L, Kumar N, Liu B Z, Shi C T, Jain J K, Samarth N, Mallouk T E and Chan M H W 2009 *Phys. Rev. Lett.* **102** 247003

[27] Deng L Z, Lv B, Wu Z, Xue Y Y, Zhang W H, Li F S, Wang L L, Ma X C, Xue Q K and Chu C W 2014 *Phys. Rev. B* **90** 214513

[28] Mizuguchi Y, Tomioka F, Tsuda S, Yamaguchi T and Takano Y 2008 *Appl. Phys. Lett.* **93** 152505

[29] Taen T, Tsuchiya Y, Nakajima Y and Tamegai T 2009 *Phys. Rev. B* **80** 092502

[30] Lei H C, Hu R W and Petrovic C 2011 *Phys. Rev. B* **84** 014520

[31] Halperin B I and Nelson D R 1979 *J. Low Temp. Phys.* **36** 599

[32] Reyren N, Tlhiel S, Caviglia A D, Kourkoutis L F, Hammer G, Richter C, Schneider C W, Kopp T, Ruetschi A S, Jaccard D, Gabay M, Muller D A, Triscone J M and Mannhart J 2007 *Science* **317** 1196

[33] Sun Y, Zhang W H, Xing Y, Li F S, Zhao Y F, Xia Z C, Wang L L, Ma X C, Xue Q K and Wang J 2014 *Sci. Rep.* **4** 6040

[34] Yeshurun Y and Malozemoff A P 1988 , *Phys. Rev. B* **60** 2202

[35] Lee H S, Bartkowiak M, Kim J S and Lee H J 2010 *Phys. Rev. B* **82** 104523

[36] Liu T J, Ke X, Qian B, Hu J, Fobes D, Vehstedt E K, Pham H, Yang J H, Fang M H, Spinu L, Schiffer P, Liu Y and Mao Z Q 2011 *Phys. Rev. B* **80** 174509

[37] Yadav A K, Thakur A D and Tomy C V 2013 *Phys. Rev. B* **87** 174524

[38] Zhang W H, Li Z, Li F S, Zhang H M, Peng J P, Tang C J, Wang Q Y, He K, Chen X, Wang L L, Ma X C and Xue Q K 2014 *Phys. Rev. B* **89** 060506(R)

[39] Bozovic I and Ahn C 2014 *Nat. Phys.* **10** 892

[40] Ge J F, Liu Z L, Liu C H, Gao C L, Qian D, Xue Q K, Liu Y and Jia J F 2015 *Nat. Mater.* **14** 285

[41] Lee J J, Schmitt F T, Moore R G, Johnston S, Cui YT, Li W, Yi W, Liu Z K, Hashimoto M, Zhang Y, Lu D H, Devereaux T P, Lee D H and Shen Z X 2014 *Nature* **515** 245